Available online at www.sciencedirect.com
ScienceDirect
Journal of Power Sources 170 (2007) 275–280
JOURNAL OF POWER SOURCES
www.elsevier.com/locate/jpowsour

Short communication

Dependence of the performance of a high-temperature polymer electrolyte fuel cell on phosphoric acid-doped polybenzimidazole ionomer content in cathode catalyst layer

Jeong-Hi Kim [a], Hyoung-Juhn Kim [b,*], Tae-Hoon Lim [b], Ho-In Lee [a,**]

[a] *School of Chemical and Biological Engineering & Research Center for Energy Conversion and Storage, Seoul National University, San 56-1 Sillim-dong, Gwanak-gu, Seoul 151-744, Republic of Korea*

[b] *Fuel Cell Research Center, Korea Institute of Science and Technology, 39-1 Hawolgok-dong, Sungbuk-gu, Seoul 136-791, Republic of Korea*

Received 19 January 2007; accepted 29 March 2007
Available online 22 April 2007

Abstract

Phosphoric acid-doped polybenzimidazole is used as a fuel cell membrane and an ionomer in the catalyst layer of a high-temperature polymer electrolyte fuel cell. Single-cell tests are performed to find the optimum ionomer content in the cathode catalyst layer. To determine the effects of the ionomer in the catalyst layer, the potential loss in the cell is separated into activation, ohmic and concentration losses. Each of these losses is examined by means of impedance and morphological analyses. With the weight ratio of ionomer to Pt/C of 1:4 (20 wt.% ionomer in catalyst layer), the fuel cell shows the lowest ohmic resistance. The activation loss in the fuel cell is lowest when the ratio is 1:9 (10 wt.% ionomer in the catalyst layer). The cell performance is dependent on this ratio, and the best cell performance is obtained with a ratio of 1:4.
© 2007 Published by Elsevier B.V.

Keywords: High-temperature polymer electrolyte fuel cell; Ionomer content; Membrane electrolyte assembly; Phosphoric acid-doped polybenzimidazole; Cathode catalyst; Potential loss

1. Introduction

The fuel cell has been put forward as one solution to the present energy crisis, because it is a safe and efficient power generation device. Among the various kinds of fuel cell, the polymer electrolyte fuel cell (PEFC) with a perfluorosulfonic acid (PFSA) polymer membrane has received a great deal of attention, due to its convenience. Nevertheless, the polymer membrane is not suitable for high-temperature operation under low humidity. Therefore, it has to be operated below 90 °C, because the proton conductivity of the polymer is dependent on the humidities of the fuel and the oxidant [1].

High-temperature fuel cell operations offer several advantages [2-6]. For example, the catalytic activity for oxygen reduction can be enhanced and the CO tolerance is improved dramatically. When a fuel cell is operated at 200 °C, even 1% CO in the reformate gas does not deteriorate the cell performance [4]. Moreover, much smaller heat-exchange and humidification systems can be employed [5]. In the case of an intermediate-temperature fuel cell, whose operation temperature is kept under 90 °C, excess water is supplied to the system to generate high proton conductivity. Therefore, a large radiator and large humidifier have to be used to ensure successful operation of the cell.

Much effort has been made to achieve good high-temperature performance of PEFCs, and remarkable progress has been achieved with acid-doped polybenzimidazoles. For example, Wainright et al. [7] proposed that poly[2,2′-(*m*-phenylene)-5,5′-bibenzimidazole] (polybenzimidazole, PBI) doped with phosphoric acid could be used for the operation of PEFCs. PBI is a basic polymer ($pK_a = 5.5$) and forms an acid–base complex when dipped in aqueous phosphoric acid, which has high proton conductivity at high temperatures. Xiao et al. [8] fabricated a PBI membrane from a polymerized mixture. A solution of PBI in polyphosphoric acid (PPA) was cast and

* Corresponding author.
** Corresponding author. Tel.: +82 2 880 7072; fax: +82 2 888 1604.
E-mail addresses: hjkim25@kist.re.kr (H.-J. Kim), hilee@snu.ac.kr (H.-I. Lee).

0378-7753/$ – see front matter © 2007 Published by Elsevier B.V.
doi:10.1016/j.jpowsour.2007.03.082

transformed into a gel by hydrolysis of the PPA. The resultant membrane retained a considerable amount of phosphoric acid, which is essential for proton conduction. Recently, Asensio et al. [9–11] reported the synthesis of poly(2,5-benzimidazole) (ABPBI) for fuel cell applications. The ABPBI can be prepared by a condensation reaction from a single commercial monomer, 3,4-diaminobenzoic acid. A direct-casting method for the production of ABPBI membranes was also developed by Kim et al. [12,13]. In the synthetic process, the monomer and the polymer are soluble in a solvent system (P_2O_5 and methanesulfonic acid), and the ABPBI membrane can be cast directly from the resulting polymerized mixture.

There have been several reports of the synthesis of PBI derivatives and their application for PEFCs [14–25]. Nevertheless, the research conducted so far has been limited to membranes, and only a few studies of electrode fabrication have been reported [14,25]. To enhance cell performance by an improvement of the platinum utilization, effective electrode fabrication is very important. This paper presents an investigation of the effects of phosphoric acid-doped PBI ionomer in the catalyst layer on single-cell performance. Especially, the ratio of ionomer to Pt/C in the cathode is varied in order to determine the optimum ionomer content for fuel cell operations.

2. Experimental

2.1. Materials

3,4-Diaminobenzoic acid (DABA, from Acros) was used after purification by a method reported previously [12]. 3,3′-Diaminobenzidine, isophthalic acid, P_2O_5, CF_3SO_3H, CH_3SO_3H, and CF_3CO_2H were purchased from Aldrich and used without further purification. A 20 wt.% Pt/C catalyst (E-tek) and carbon paper (Toray TGPH-090) were used for the fabrication of the membrane–electrode assembly (MEA).

2.2. Preparation of ABPBI membrane

As described by Kim et al. [12], purified 3,4-diaminobenzoic acid was polymerized in a reaction medium composed of P_2O_5 and CH_3SO_3H. The polymer solution was poured on to a glass plate and flattened by an adjustable doctor blade to obtain a uniform thickness. It was then immersed in a water bath and detached from the glass plate. The residual acid in the polymer film was extracted by neutralization with ammonium hydroxide solution to make a de-doped ABPBI film. This film was washed and dried at 80 °C under reduced pressure for 2 days. It was then immersed in 50 wt.% aqueous phosphoric acid for 5 days to produce a phosphoric acid-doped ABPBI membrane.

2.3. Preparation of PBI polymer powder

3,3′-Diaminobenzidine and isophthalic acid were dissolved in a mixture of P_2O_5, CF_3SO_3H, and CH_3SO_3H [13] and reacted at 150 °C for 30 min. The viscous polymer solution was poured into water to produce a wire-like polymer. The polymer was washed with water and neutralized with ammonium hydroxide solution to obtain de-doped PBI powder. The PBI powder was dried at 80 °C under reduced pressure. It was used as a binding ionomer for fabrication of electrodes.

2.4. Preparation of the electrode

A Pt catalyst slurry was prepared by the method described by Kim et al. [13]. The slurry was coated on a carbon fibre paper using an adjustable doctor blade, and then dried at room temperature to produce an ionomer-impregnated catalyst-coated electrode. The amount of H_3PO_4 doped into PBI was fixed at six H_3PO_4 molecules per PBI repeating unit. The weight percentage of H_3PO_4-doped PBI in the catalyst layer ranged from 5 to 40 wt.% and hereafter is termed IC.

2.5. Characterization of catalyst layer

The surface morphology of the catalyst layer was examined with a scanning electron microscope (SEM; Hitachi, S-4200). The BET surface area, pore volume and pore-size distribution were measured by means of the nitrogen adsorption–desorption method using a Micromeritics ASAP 2010 instrument.

The metallic surface area was analyzed by a CO chemisorption apparatus (Micromeritics, ASAP 2010C). For the analysis, the sample was pretreated at 200 °C under reduced pressure and then cooled to room temperature.

2.6. Single-cell performance test

The catalyst-coated electrodes and phosphoric acid-doped ABPBI membrane (thickness: 105 ± 5 μm) were assembled to produce the MEA, without any hot-pressing process. The IC of the anode was fixed at 25 wt.%. The active area of the single cell was 2 cm^2. The Pt loadings of the cathode and anode were 0.40 ± 0.05 and 0.55 ± 0.05 mg cm^{-2}, respectively.

Hydrogen was used as a fuel and oxygen or air as an oxidant, without external humidification, and the cell temperature was kept at 150 °C. Polarization curves were obtained using an electric loader (Daegil Electronics, EL500P). Impedance spectra were plotted using a potentiostat (Zahner, IM6) at different current densities in the frequency range of 100 kHz to 0.1 Hz. The specific ohmic resistance was obtained from the impedance curve.

3. Results and discussion

The IC in the cathode was varied from 5 to 40 wt.% to find the optimum value for high-temperature PEFC operation. The single-cell performances with various ICs in the cathode catalyst layer are presented in Fig. 1. The performance increases as the IC increased from 5 to 20 wt.%. However, it decreases as the IC increased from 20 to 40 wt.%.

The ohmic resistances of the MEAs with different IC values obtained from a potentiostat in galvanostatic mode are presented in Fig. 2. The ohmic resistance is a minimum when the IC is 20 wt.%. Considering that the ohmic resistance is a function

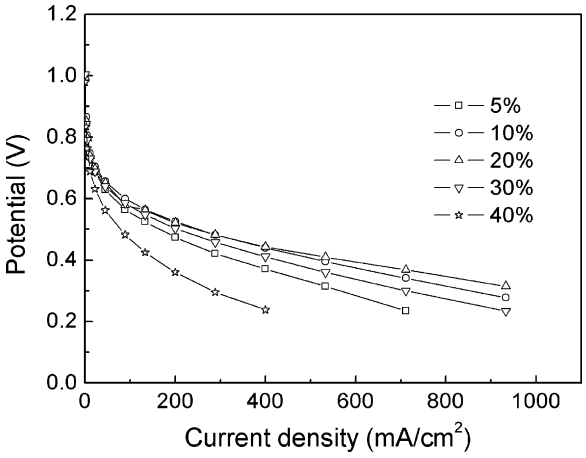

Fig. 1. Polarization curves with various ICs in cathode catalyst layer at 150 °C using dry H_2/O_2 feed.

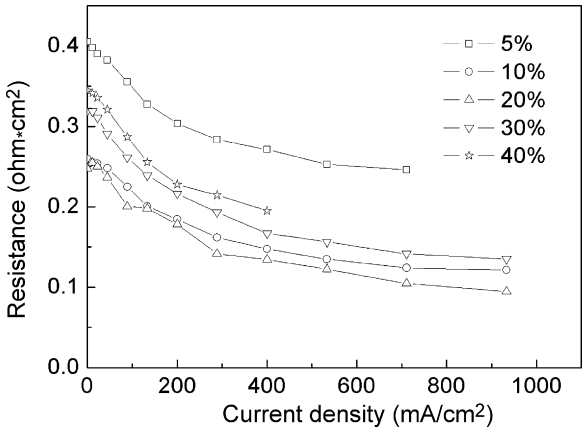

Fig. 2. Ohmic resistances at 150 °C using dry H_2/O_2 feed with various ICs in cathode catalyst layer.

of both the ionic conduction afforded by the ionomer and the electronic conduction afforded by the catalyst, the observed minimum resistance is considered to result from an optimum balance between the ionic and electronic conductivities. The high resistance obtained with IC = 5 wt.% is due to poor connection of the ionomer, whereas the high resistance with IC = 40 wt.% is due to a decrease in electronic connection caused by hindrance afforded by the ionomer around the catalyst particles.

Morphological changes in the catalyst layers with different ionomer contents are presented in Fig. 3. An increase in the degree of interconnection among the catalyst particles and a decrease in pore volume are observed as the ionomer content increased.

The pore-size distributions of the catalyst layers with different ionomer contents are presented in Fig. 4. As the ionomer content is increased in the catalyst layer, the numbers of primary and secondary pores decrease. This behaviour is different from

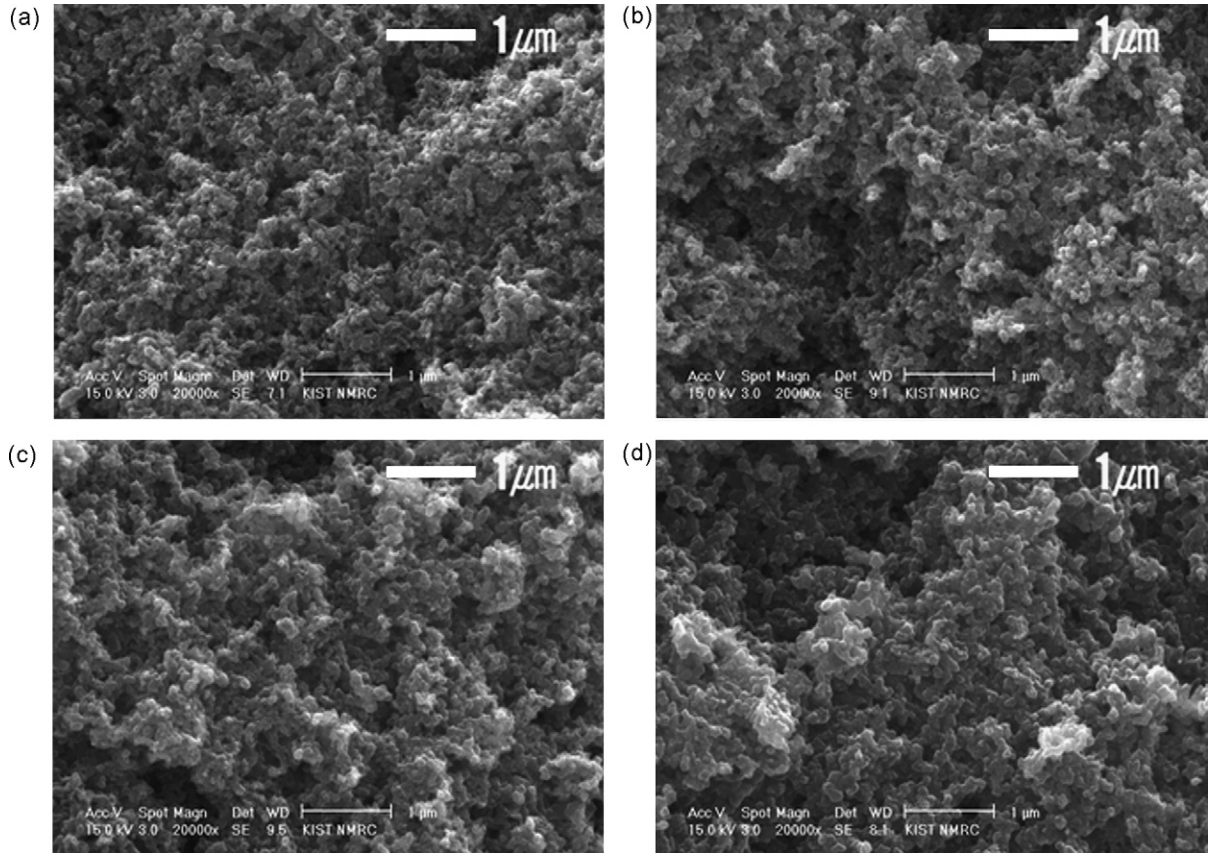

Fig. 3. Scanning electron micrographs of catalyst layer with different ICs of (a) 10 wt.%, (b) 20 wt.%, (c) 30 wt.%, and (d) 40 wt.%.

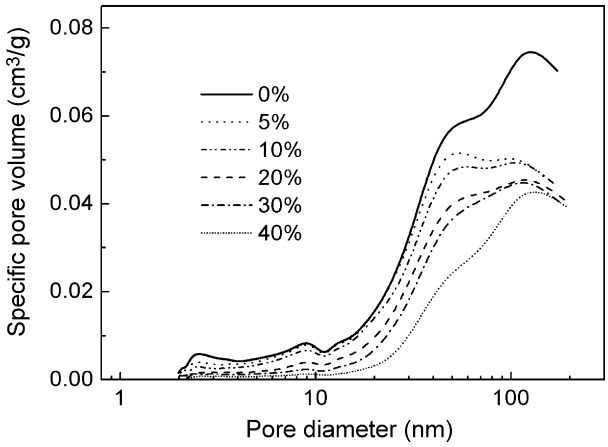

Fig. 4. Pore-size distributions of catalyst layer with various ICs.

that of the Nafion-type binder system used for intermediate-temperature PEFCs [26–28]. In this case, the primary pore volume remains constant, even with an increase of the Nafion ionomer content in the catalyst layer. This difference can be related to the state of the binders during fabrication of the electrode. The phosphoric acid-doped PBI binder is in the solution state, whereas the Nafion binder exists as a colloidal state. Thus, phosphoric acid-doped PBI binder can penetrate into the primary pores whereas the colloidal Nafion cannot.

The relative exposures of the platinum surface with the different IC values were analyzed in terms of CO chemisorption. By assuming a stoichiometry of one CO molecule per Pt atom on the surface, the platinum metallic surface area was calculated from the amount of CO adsorbed. Then, the relative exposure was calculated as the ratio of the metallic surface area of the sample with IC = x wt.% to that with IC = 0 wt.% (no ionomer impregnation).

The relative exposures of the platinum surface with the various ICs are shown in Fig. 5. A severe decrease in the relative exposure is observed initially, as the ionomer content is increased. The decrease becomes more gradual above IC = 20 wt.%.

In order to obtain a better understanding of the effect of the ionomer content in the cathode on the performance, the polarization curves were analyzed using the three loss factors, viz, activation, ohmic and concentration losses, as follows [29]:

$$V = E_{\text{thermo}} - \eta_{\text{total}}$$
$$= E_{\text{thermo}} - (\Delta V_{\text{cross}} + \eta_{\text{act}} + \eta_{\text{ohmic}} + \eta_{\text{conc}})$$

where V is the measured potential of the fuel cell; E_{thermo} the thermodynamically predicted ideal potential, 1.15 V at 150 °C; η_{total} the total potential loss; ΔV_{cross} the potential drop due to cross-over through the membrane; η_{act} the activation loss due to reaction kinetics; η_{ohmic} the ohmic loss from ionic and electronic resistances; and η_{conc} is the concentration loss due to mass transfer.

The η_{act} was calculated from the Tafel equation using the performance data at low current densities and η_{ohmic} was calculated by multiplying the specific ohmic resistance by the current density in each case. Then, η_{conc} was obtained by subtracting η_{act} and η_{ohmic} from η_{total}. The difference in cell voltage between operations with H_2/O_2 and H_2/air, which is referred to as the oxygen gain, was used to confirm the effect of the ionomer content on the concentration loss.

For exact evaluation of the effect of the electrodes with different IC values on the cell performance, excluding cross-over through the membrane, all of the measured open-circuit voltages (OCVs) were fitted to 1.15 V and the potential difference between 1.15 and the measured OCV was added to all of the potential data. The variation in the activation loss with the IC value in the cathode catalyst layer at low current densities is presented in Fig. 6. It is a minimum for IC between 10 and 20 wt.% regardless of the current density. The variation of the ohmic loss with the IC value in the cathode catalyst layer is presented in Fig. 7. As expected from the results shown in Fig. 2, the ohmic loss is lowest at IC = 20 wt.%. The concentration loss due to mass transport is presented in Fig. 8. It increases as the ionomer content increases, due to an increase in the mass transport resistances of oxygen and water vapour in the narrow pore volume. Among the three losses (activation, ohmic, concentration), the activation loss is the main contributor to the total loss in fuel cell performance. The concentration loss exhibits good

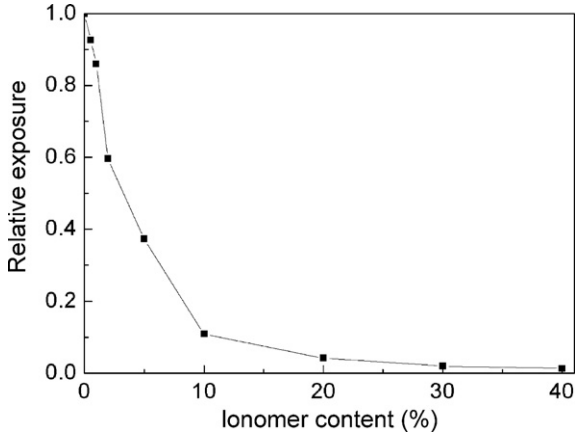

Fig. 5. Relative exposures of platinum surface with various ICs.

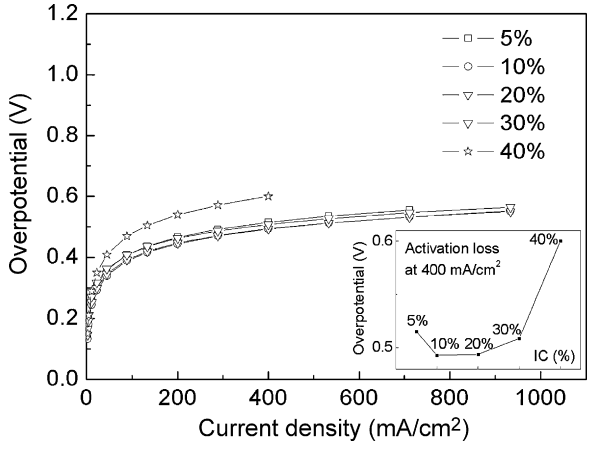

Fig. 6. Relationship between activation loss and current density with various ICs in cathode catalyst layer.

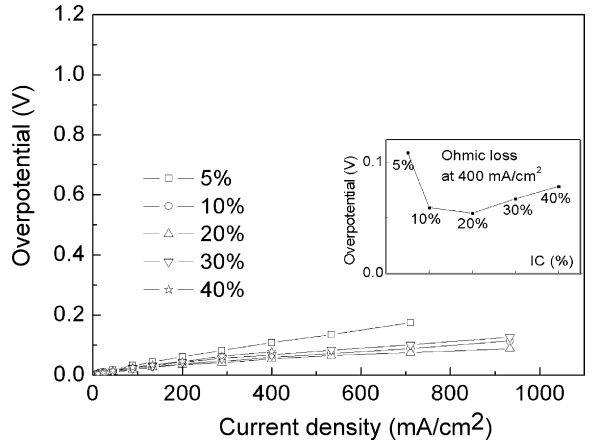

Fig. 7. Relationship between ohmic loss and current density with various ICs in cathode catalyst layer.

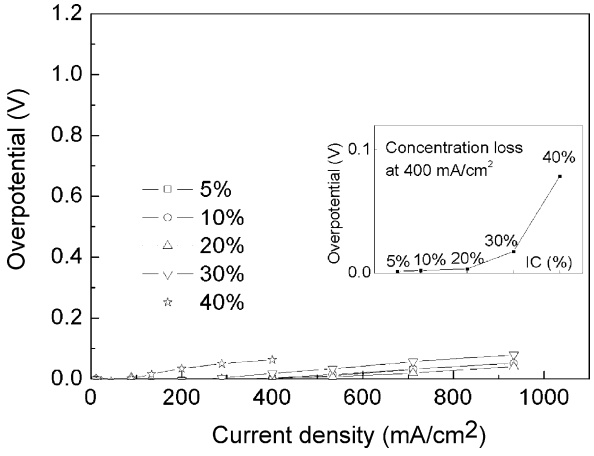

Fig. 8. Relationship between concentration loss and current density with various ICs in cathode catalyst layer.

agreement with the oxygen gain presented in Fig. 9. From the potential differences between operations with H_2/O_2 feed and H_2/air feed, an increase in the mass transport resistance with increasing ionomer content is conformed.

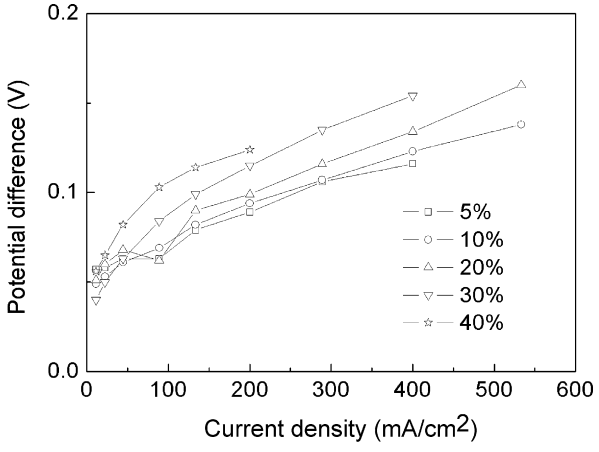

Fig. 9. Relationship between oxygen gain and current density with various ICs in cathode catalyst layer.

4. Conclusions

Phosphoric acid-doped polybenzimidazole has been used as an ionomer in the catalyst layer of a high-temperature polymer electrolyte fuel cell. The ratio of ionomer to Pt/C in the cathode is varied to determine the optimum ionomer content for fuel cell operation. This is found to be 20 wt.% (ratio of ionomer to Pt/C = 1:4) for PEMFC operation. With separation of the total potential loss into activation, ohmic and concentration losses, a better understanding of the influence of the ionomer in the cathode catalyst layer on cell performance is obtained. The activation loss is the main contributor to the total potential loss. The high activation loss is due to the penetration of the PBI-phosphoric acid ionomer into both the primary and secondary pores that results in low utilization of the platinum catalyst.

Acknowledgements

This work was financially supported by the Fuel Cell Research Center of Korea Institute of Science and Technology and by the ERC Program of MOST/KOSEF (Grant no. R11-2002-102-00000-0).

References

[1] J.S. Wainright, M.H. Litt, R.F. Savinell, in: W. Vielstichm, A. Lamm, H.A. Gasteiger (Eds.), Handbook of Fuel Cells, vol. 3, John Wiley & Sons Inc., UK, 2003, pp. 436–446.
[2] D. Weng, J.S. Wainright, U. Landau, R.F. Savinell, J. Electrochem. Soc. 143 (1996) 1260–1263.
[3] Y.M. Kim, S.H. Choi, H.C. Lee, M.Z. Hong, K. Kim, H.-I. Lee, Electrochim. Acta 49 (2004) 4787–4796.
[4] C. Pan, R. He, Q. Li, J.O. Jensen, N.J. Bjerrum, H.A. Hjulmand, A.B. Jensen, J. Power Sources 145 (2005) 392–398.
[5] Q. Li, R. He, R.W. Berg, H.A. Hjuler, N.J. Bjerrum, Solid State Ionics 168 (2004) 177–185.
[6] H.-J. Kim, T.-H. Lim, J. Ind. Eng. Chem. 10 (2004) 1081–1085.
[7] J.S. Wainright, J.-T. Wang, D. Weng, R.F. Savinell, M. Litt, J. Electrochem. Soc. 142 (1995) L121–L123.
[8] L. Xiao, H. Zhang, E. Scanlon, L.S. Ramanathan, E.-W. Choe, D. Rogers, T. Apple, B.C. Benicewicz, Chem. Mater. 17 (2005) 5328–5333.
[9] J.A. Asensio, S. Borrós, P. Gómez-Romero, J. Membr. Sci. 241 (2004) 89–93.
[10] J.A. Asensio, S. Borrós, P. Gómez-Romero, J. Electrochem. Soc. 151 (2004) A304–A310.
[11] J.A. Asensio, P. Gómez-Romero, Fuel Cells 5 (2005) 336–343.
[12] H.-J. Kim, S.Y. Cho, S.J. An, Y.C. Eun, J.-Y. Kim, H.-K. Yoon, H.-J. Kweon, K.H. Yew, Macromol. Rapid Commun. 25 (2004) 894–897.
[13] H.-J. Kim, S.J. An, J.-Y. Kim, J.K. Moon, S.Y. Cho, Y.C. Eun, H.-K. Yoon, Y.M. Park, H.-J. Kweon, E.-M. Shin, Macromol. Rapid Commun. 25 (2004) 1410–1413.
[14] J.-T. Wang, R.F. Savinell, J. Wainright, M. Litt, H. Yu, Electrochim. Acta 41 (1996) 193–197.
[15] J.-T. Wang, J.S. Wainright, R.F. Savinell, M. Litt, J. Appl. Electrochem. 26 (1996) 751–756.
[16] J.J. Fontanella, M.C. Wintersgill, J.S. Wainright, R.F. Savinell, M. Litt, Electrochim. Acta 43 (1998) 1289–1294.
[17] Q. Li, H.A. Hjuler, N.J. Bjerrum, Electrochim. Acta 45 (2000) 4219–4226.
[18] O. Savadogo, B. Xing, J. New Mater. Electrochem. Syst. 3 (2000) 345–349.
[19] Q. Li, H.A. Hjuler, N.J. Bjerrum, J. Appl. Electrochem. 31 (2001) 773–779.
[20] Q. Li, R. He, J. Gao, J.O. Jensen, N.J. Bjerrum, J. Electrochem. Soc. 150 (2003) A1599–A1605.
[21] Q. Li, R. He, J.O. Jensen, N.J. Bjerrum, Fuel Cells 4 (2004) 147–159.

[22] J.O. Jensen, Q. Li, R. He, C. Pan, N.J. Bjerrum, J. Alloys Compd. 404 (2005) 653–656.
[23] Y.-L. Ma, J.S. Wainright, M.H. Litt, R.F. Savinell, J. Electrochem. Soc. 151 (2004) A8–A16.
[24] F. Seland, T. Berning, B. Børresen, R. Tunold, J. Power Sources 160 (2006) 27–36.
[25] J. Lobato, M.A. Rodrigo, J.J. Linares, K. Scott, J. Power Sources 157 (2006) 284–292.
[26] M. Uchida, Y. Aoyama, N. Eda, A. Ohta, J. Electrochem. Soc. 142 (1995) 463–468.
[27] M. Uchida, Y. Aoyama, N. Eda, A. Ohta, J. Electrochem. Soc. 142 (1995) 4143–4149.
[28] J.-H. Kim, H.Y. Ha, I.-H. Oh, S.-A. Hong, H.-N. Kim, H.-I. Lee, Electrochim. Acta 50 (2004) 797–802.
[29] R.P. O'Hayre, S.-W. Cha, W. Colella, F.B. Prinz, Fuel Cell Fundamentals, John Wiley & Sons Inc., New Jersey, 2006, pp. 169–173.